4TH INTERNATIONAL CONFERENCE ON KNOWLEDGE & INNOVATION IN ENGINEERING, SCIENCE & TECHNOLOGY
21-23 December, 2018
Berlin - Germany

Numerical Modelling and Validation of Vibratory Trough for Surface Finishing

Govind Gour[1], Zhang Jing[1], Pulkit Kapur[1], Indira Khadka[1], Tegoeh Tjahjowidodo[2], Swee Hock Yeo[2] and Sylvie Castagne[3]

[1]Rolls-Royce@NTU Corporate Lab, c/o School of Mechanical & Aerospace Engineering,

Nanyang Technological University, 50 Nanyang Avenue, Singapore 6397981

[2]School of Mechanical and Aerospace Engineering, Nanyang Technological University,

50 Nanyang Avenue, Singapore 6397981

[3]Department of Mechanical Engineering, KU Leuven, Leuven, 3001, Belgium;

Member Flanders Make, Leuven, Belgium

Abstract

The vibratory surface finishing process has been an integral part of the manufacturing domain to perform post manufacturing process such as deburring edges, removal of unnecessary material, improving the life cycle of the component via suppressing the surface deformities such as reducing surface roughness. The current research investigates the vibrational response of the vibratory trough under various frequencies. A tri-axial piezoelectric accelerometer along with data acquisition tool (DAQ) is used to measure acceleration on the various positions on the vibratory trough. The measurements indicated that frequency is same throughout the trough however the amplitude varies on the various location of the trough. Furthermore, ABAQUS/Explicit is used develop the numerical model of the vibratory trough to investigate the response under various input frequencies. The numerical results corroborated the experimental measurements and these findings can further be extended to optimize the vibratory surface finish process.

Keywords: vibratory finishing, vibropolishing, surface roughness, finite element modelling

Introduction

Vibropolishing also known as vibratory finishing, is a type of mass finishing manufacturing process that allow various workpieces to be treated simultaneously. The aim of this process is to deburr, radius, clean, descale, polish, burnish and brighten the workpiece (L. K. Gillespie, 2007). The finishing process creates grinding contact between media and component surface, and results in achieving the desired surface polishing needs in relatively low-cost way. Although vibropolishing has been employed in many applications, especially in aerospace industry to attain the surface roughness of airfoils as required, the detailed mechanisms and key process variables are still less known.

Media is an abrasive element used in vibropolishing process. A great variety of media is currently available in the market to provide a large range of capability in vibropolishing process. The functions of media are designed mainly for cutting, luster, part separation and surface scrubbing. Media is built up by different types of binders and different solid particles of materials and shapes. To make the conditions of media flow consistent, lubricants such as water play a role in removing burrs.

Cutting can remove burrs and smoothen surfaces. Large abrasive grains inside media increase the impact force during media hitting on the component effectively. Some kinds of media are designed to increase luster on the surface of workpiece. The abrasiveness between media and workpiece is at a very low level. Controlling the degree of surface abrasiveness by selecting suitable media, can help in surface condition characterization of the workpiece. When component undergoes cutting, deburring or burnishing processes, function of separate parts of the media plays an important role. The value of part-on-part contact is decided by the volume ratio between media and component. Surface scrubbing is a common ability of media. With the assistance of lubricant, scale and residues can be removed and designated surface properties can be achieved (DeGarmo, 2003).

Currently vibratory machines are the most commonly used mass finishing equipment in industry among centrifugal disks, vibratory machines and tumbling machines. Vibratory machines have been used in industry for more than five decades now. In the vibropolishing process, the kinetic energy of the vibrational walls is received from the rotation of eccentric mass; the media inside is excited by vibrational wall and will form a granular flow with relative patterns, and then vibrational energy is transferred from media flow to the surfaces of components. The surface condition of workpiece is decided by this energy transfer mechanism.

Due to different requirements of surface properties of workpieces, different kinds of vibropolishing machines have been designed. As shown in Figure.1(a), the bowl-polisher has tri-axial vibration. Due to the rotation of eccentric mass, the pattern of media flow is combined vertical roll and horizontal slide and results in a helical and spiral motion (Nebiolo, 2017). Additionally, a trough-polisher can be found in Figure.1(b). According to different requirements, both machines can be developed in different sizes, frequencies and amplitudes of vibration. The amplitude and frequency of vibration, lubricant and media are the key parameters in vibropolishing process which are mainly responsible for the surface properties of workpiece.

Figure 1: Two types of vibropolishing system: (a) bowl-polisher; (b) trough-polisher

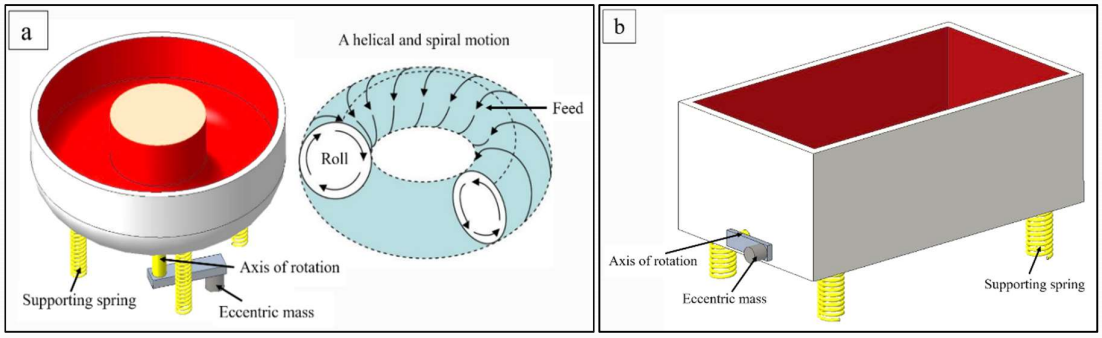

Although vibropolishing has been employed for over fifty years, the process characteristics, such as dynamic response of vibropolishing machine, media flow and the mechanics of interaction between media and workpiece, are less known. The field of material removal and vibrator deburring (Domblesky et al., 2003; Domblesky et al., 2004; L. R. K. Gillespie, 1975; Sofronas & Taraman, 1979) and the media-workpiece contact force (Hashimoto et al., 2016; Yabuki et al., 2002) have been studied in some experiments, but the fundamental understanding of vibropolishing processes is still weak. This paper emphasizes on using accelerometer and data acquisition tools to find the dynamic response of empty vibratory machine under various motor frequencies, and develop a numerical model to investigate the machine's response to vibrational load.

Experimental Setup

The vibratory finishing machine mainly consists of the container (bowl or trough) attached with the vibratory motor, media (with optional lubricant) and component. Figure 2 shows the schematic of the vibratory trough which is used in this work.

Figure 2. Schematic of the vibratory trough

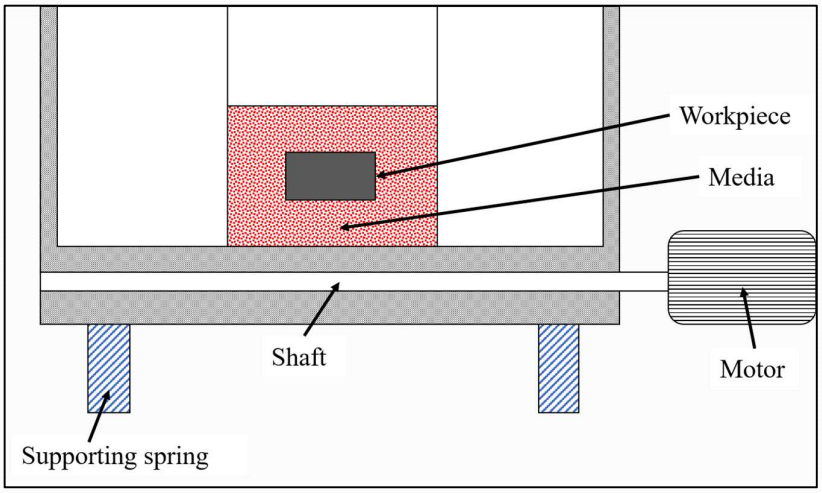

The vibratory mechanism of the machine is also illustrated in Figure 2. The motor attached to the vibratory trough drives the shaft, which is mounted under the trough and connected to the motor using a flexible joint. The eccentric mass is mounted to the shaft. When the motor is switched on, rotational eccentric mass generates eccentric force. Due to the constraints of the springs attached to trough, the whole machine vibrates synchronously.

Accelerometer can be used to obtain the acceleration value of vibratory trough at various points, and data acquisition tools can be used to convert acceleration data to displacement and vibration frequency data using Fast Fourier Transformation (FFT). It is reasonable to use accelerometer as the main sensor in this study to identify the dynamic response of empty trough. As shown in Figure 3, a Meggitt tri-axial isotron accelerometer (integrated electronic piezoelectric (IEPE) sensor) is chosen to measure the accelerations at various locations in the vibratory trough. The sensitivities of the accelerometer in tri-axes are 4.808 mV/g in x-axis, 5.005 mV/g in y-axis and 5.208 mV/g in z-axis. The range of frequency for the accelerometer is from 0 Hz to 5000 Hz. A Dytran E4114B1 amplifier is adopted to supply a 2mA current to the accelerometer for collecting acceleration signal. Adlink USB-2405(G) system is selected to receive vibrational data and subsequent signal processing. It can support the Meggitt tri-axial isotron accelerometer and provide four channel input samples with sampling rate at 128 kS/s simultaneously. Visual Signal DAQ Express is used as the compatible software to display acceleration and frequency data in real time and perform a time-frequency spectrum analysis.

The arrangement of accelerometer and DAQ in the vibratory trough is shown in Figure 4. The tri-axial accelerometer was adhered tightly to the various locations of the vibratory trough using petro- wax. The acceleration and the frequency data after FFT analysis by the DAQ system is recorded and exported to Microsoft Excel format. During signal data processing, the acceleration is converted into displacement for comparison with numerical results.

Figure 3. Accelerometer and other data acquisition tools

Figure 4: The arrangement of accelerometer and DAQ in vibratory trough

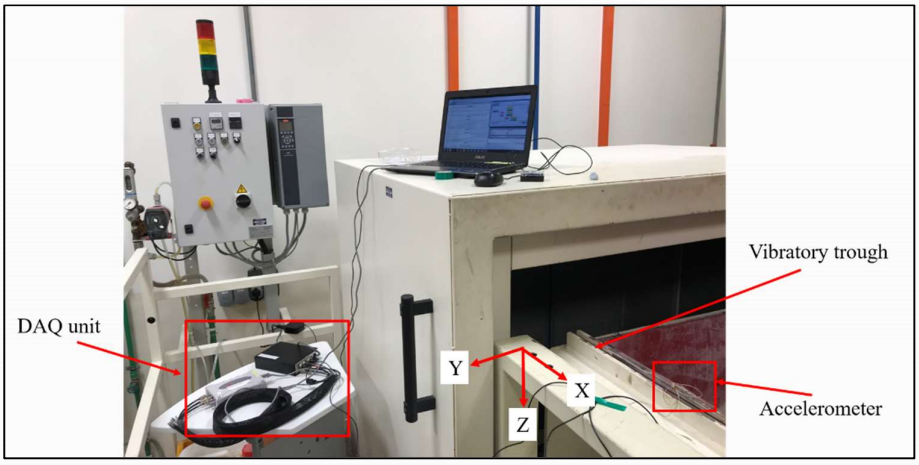

Numerical Modelling

Based on experimental setup, the numerical simulation is done in ABAQUS. The numerical model of vibratory trough consists of polyurethane (PU) inner layer and steel outer casing combined by tie constraint. The material properties for PU and steel are shown in Table 1.

Table 1. Mechanical properties of PU and Steel

Material properties	Polyurethane	Steel
Density (Kg/m^3)	1150	7890
Young's modulus (GPa)	1.5	210
Poisson's ratio	0.3	0.42

Supporting springs are attached to the bottom of the model to constrain the motion of the trough. The material of spring is 65Si7 obtained from literature (Arora et al., 2014). The mechanical properties of 65Si7 are listed at Table 2.

Table 2. Mechanical properties of spring

Mechanical property	Young's modulus (E)	BHN	Poisson's ratio	Tensile strength ultimate	Tensile strength yield	Elongation at fracture	Density
Value	200 GPa	380-432	0.266	1.27 GPa	1.08 GPa	7%	7850 Kg/m3

The stiffness of spring is calculated using information manual of trough and mechanical properties of spring. The mesh method ("Abaqus Analysis User's Manual (6.13),") used to discretize the trough and details of element is listed in Table 3.

Table 3. Basic information of mesh

Element Type	Geometric order	Element shape	Global seeds	Total No. of elements
C3D10	Quadratic	Tetrahedral	100 mm	21609

The centrifugal forces induced by eccentric mass have been calculated based on the input rotation of motor and dimension of eccentric mass. The calculated forces are applied as concentrated forces on the connect points which are at same locations as in experimental measurements.

Table 4. Identify the centrifugal force as input load

Parameters	Expression and value
Centrifugal force F_Y	$m\omega^2 r*\sin(\omega t)$
Centrifugal force F_Z	$m\omega^2 r*\cos(\omega t)$
Input frequency	24.93 Hz
Eccentric mass (m)	340Kg
Approximated radius of eccentric mass (r)	100mm
Angular speed (ω)	156.661rad/s

Results and Discussion

The experimental trials have been carried on to the vibratory trough. The tri-axial acceleration data around the corners and at the middle points of the edges is taken and compared, which is shown in Figure 5. The acceleration curves expound similar vibratory pattern at all points. The vibratory frequency of the trough is 23.46 Hz and is evenly distributed throughout the trough. The measurement results prove that the vibratory trough is under an axisymmetric condition. For finalizing the measurement points, a quadrant of the trough can be taken to analyze the vibration response of the trough. Total 28 points were created on the quadrant to measure acceleration data. The results indicate similar frequency throughout the trough, however, the amplitude or displacement is found to be varied based on the location.

Figure 6 describes the acceleration data measured from the top and bottom regions of the vibratory trough. At the top region of the trough, as shown in Figure 6(a), the acceleration curves illustrate vibratory amplitude domination in Z-direction (namely depth of the trough); the acceleration values in X and Y directions are relatively low as compared to Z-direction and can be neglected. It can be inferred that the motion at top region of trough is almost pure translation in Z-direction; translations in X & Y directions and rotation along X-direction are negligible. Along the length of the top edge (along X-direction), all points have the similar vibratory pattern. Converting the acceleration values to displacement values, the amplitude of displacement in Z-direction is found to be around 3.4 mm, but the value is around 0.25 mm for X and Y directions.

Figure 5: The acceleration data around the corners and at the middle points of trough

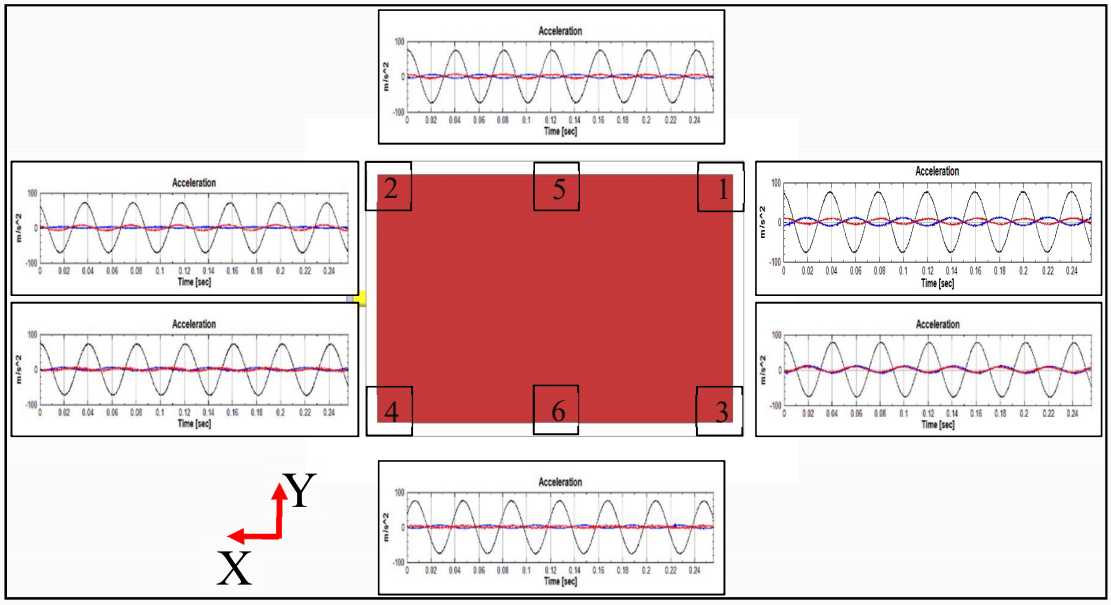

At the bottom region of the trough shown in Figure 6 (b), the acceleration curves illustrate that: The vibratory amplitude is dominating both in Y and Z directions (namely width and depth of the trough). The amplitude of acceleration in Y-direction is slightly higher than Z-direction; The acceleration values in X directions are relatively low as compared to Y and Z directions and can be neglected. It means that the motion at bottom region of the trough is a combined translation in Y & Z directions and rotation along X-direction; translations in X-direction are negligible. Along the length of bottom edge (along X-direction), all points show similar vibratory pattern. Converting the acceleration value to displacement value, amplitude of displacement is found to be around 3.6 mm in Y-direction, around 2.8 mm in Z-direction, and the value is only 0.15 mm in X-direction. Hence it can be inferred from the experimental data that the vibratory trough is vibrating in two-axes (Y & Z) while the motion in X-direction is negligible.

Initial numerical investigation indicated that the trough's motion is close to rigid body (does not undergo any deformation) and does not indicate any influence of increased number of elements. To understand the influence of the mesh method, the mesh is further refined on trough. The type and geometric order of the element are kept similar as previous numerical approach except the number of elements. The total number of tetrahedral elements were close to 200,000. The numerical displacement on two points namely: bottom and top point is measured. The bottom point at all input frequencies (23.46 Hz, 15.64Hz and 11.73Hz) indicated similar trend and amount of displacement as observed in the experiments.

Figure 7 shows the comparison between numerical and experimental displacement of both top and bottom points at the input frequency of 23.46 Hz.

Figure 6. The acceleration data at the (a) top and (b) bottom regions of the trough

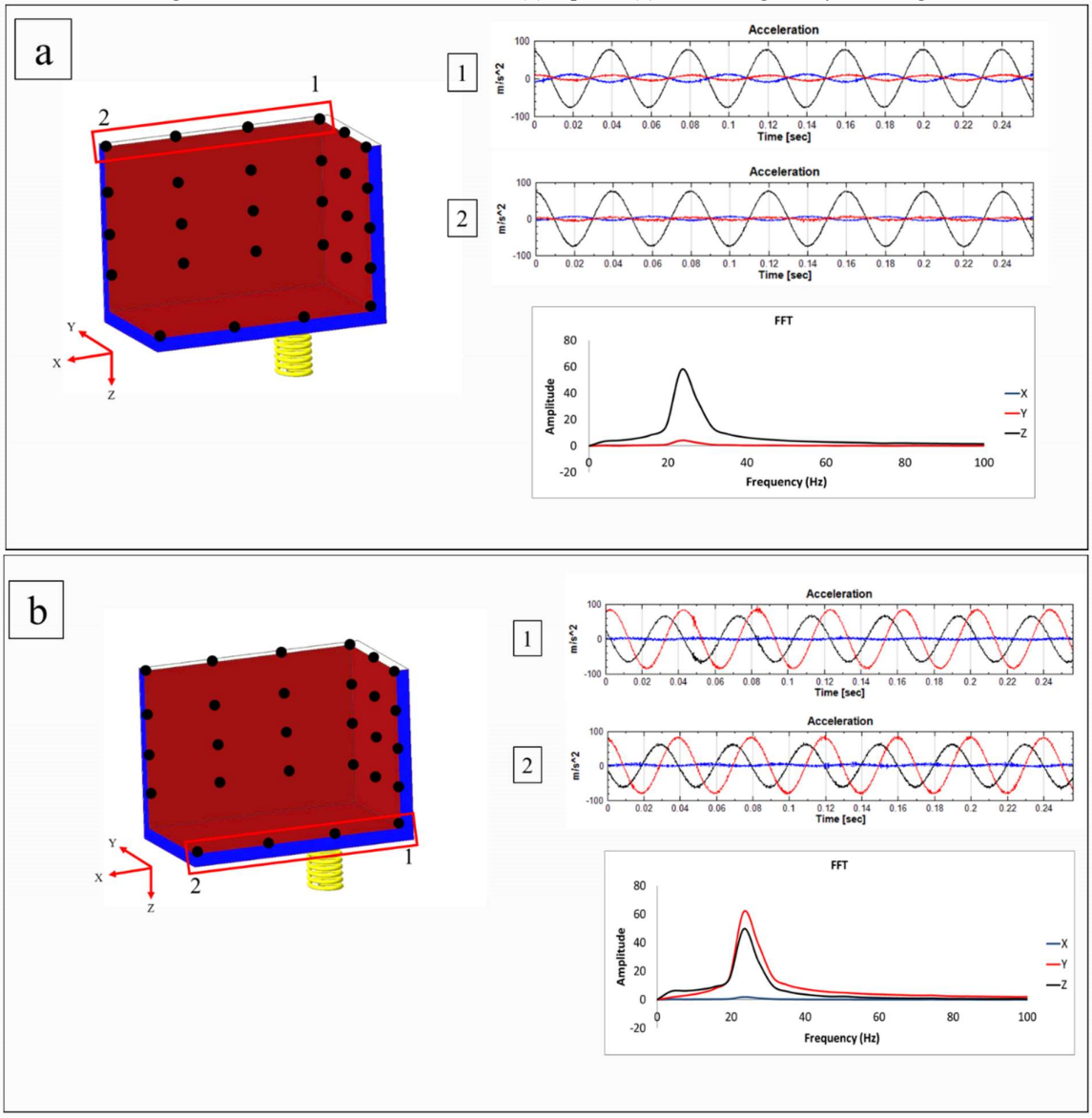

Figure 7. Comparison between Numerical and Experimental Data for Trough Displacement

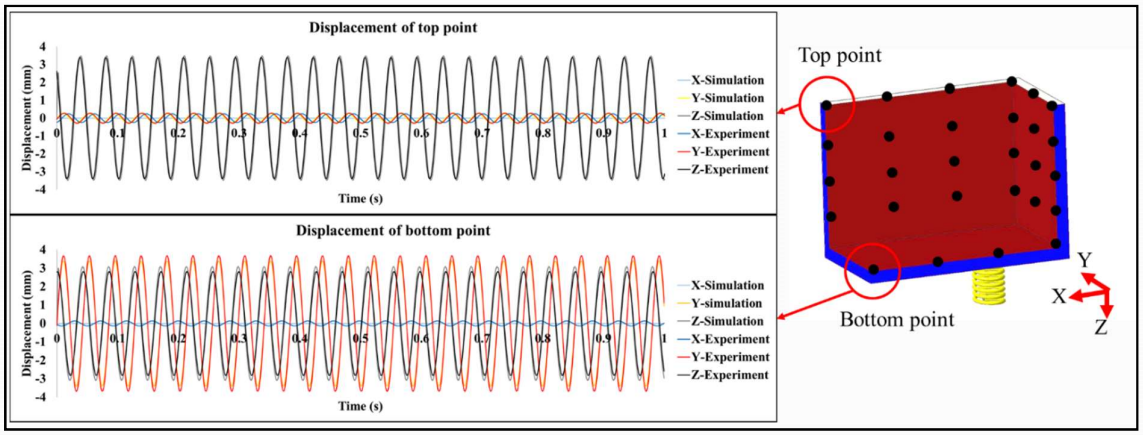

Additionally, it can be seen from the acceleration curves that the acceleration values in Y-direction increase along Z-direction (along the depth of trough). It may be due to the configurations of eccentric mass and springs. The increasing trend of displacement amplitude in Y-direction is shown in Figure 8. Also, the numerical amplitude of displacement agrees well with experimental value. It can be understood that the bottom part of the trough is more energetic as there two major displacements/amplitude (in Z and Y directions) were noted in contrast with the top part which had displacement/amplitude only in Z-direction. This result can further help in improving the performance of surface polishing of the component.

Figure 8. Increasing trend of displacement amplitude along tri-axes

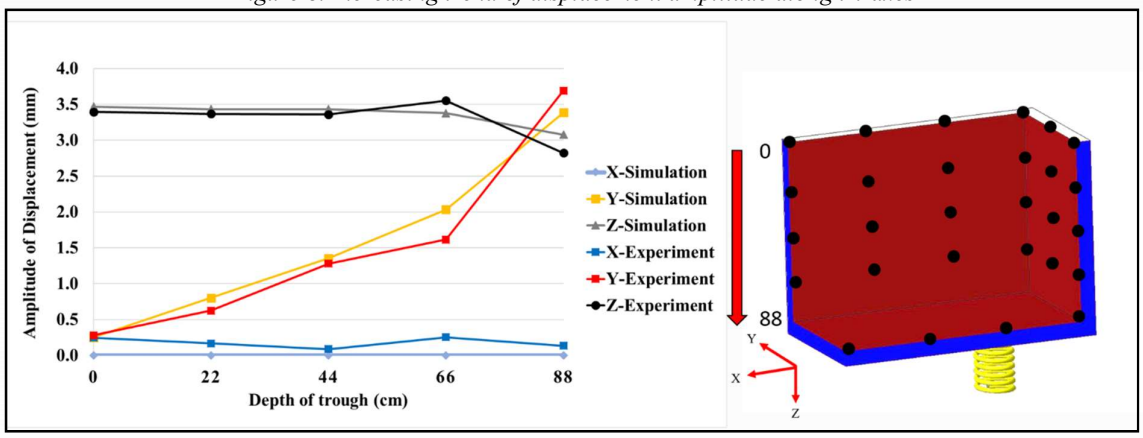

Conclusion

- In the overall measurements, the displacement in Z-direction (along the depth) is found to more dominant than in other two directions. However, at the bottom part of trough, significant displacement in the Y-direction (lateral) is observed as well.
- The findings revealed that bottom part of the trough is found to be more energetic as there were two major displacements/amplitudes in Z and Y directions, which further can lead to better performance in surface finishing and peening of the component.
- Initial numerical investigation indicated that the trough's motion is close to rigid body, which does not undergo any plastic deformation and there is no influence observed by increasing the number of elements.
- The numerical displacements on two points, at both bottom and top of the trough, are measured. The numerical results at all input frequencies indicate similar trend and amount of displacement as observed in the experiments.
- Overall, the FEM analysis conducted on the trough also affirms high displacement at the bottom part of the trough and corresponds well with experimental trends. The simulated vibration indicates a higher process rate at the bottom of the trough.

Acknowledgment

This work was conducted within the Rolls-Royce@NTU Corporate Lab with support from the National Research Foundation (NRF) Singapore under the Corp Lab@University Scheme. The authors would like to thank Mr Kunal AHLUWALIA and his team in assisting with their sensors and DAQ tools to carry out the experiments.

References

- Gillespie, L. K. (2007). *Mass finishing handbook*: New York : Industrial Press, c2007. 1st ed.
- DeGarmo, E. P. (2003). *Materials and processes in manufacturing*: New York : Wiley, c2003. 9th ed.
- Nebiolo, W. P. (2017). Calculating Applied Media Force During Vibratory Finishing. *Products Finishing, 81*(8), 28-31.
- Domblesky, J., Cariapa, V., & Evans, R. (2003). Investigation of vibratory bowl finishing. *International Journal of Production Research, 41*(16), 3943-3953.
- Domblesky, J., Evans, R., & Cariapa, V. (2004). Material removal model for vibratory finishing. *International Journal of Production Research, 42*(5), 1029-1041.
- Gillespie, L. R. K. (1975). A quantitative approach to vibratory deburring effectiveness. *SME Tech. Report.*
- Sofronas, A., & Taraman, S. (1979). Model development and optimization of vibratory finishing process. *International Journal of Production Research, 17*(1), 23.
- Hashimoto, F., Johnson, S. P., & Chaudhari, R. G. (2016). Modeling of material removal mechanism in vibratory finishing process. In (Vol. 65, pp. 325-328).
- Yabuki, A., Baghbanan, M. R., & Spelt, J. K. (2002). Contact forces and mechanisms in a vibratory finisher. In (Vol. 252, pp. 635-643).
- Arora, V. K., Bhushan, G., & Aggarwal, M. L. (2014). Effect of Assembly Stresses on Fatigue Life of Symmetrical 65Si7 Leaf Springs. *ISRN Otolaryngology*, 1-10. doi:10.1155/2014/762561
- Abaqus Analysis User's Manual (6.13). Retrieved from http://abaqus.software.polimi.it/v6.12/books/usb/default.htm?startat=pt06ch28s01ael03.html